

**STRUCTURAL OPTIMIZATION OF THIN WALLED SEMI-MONOCOQUE
WING STRUCTURES USING DIFFERENT TYPES OF FINITE
ELEMENTS IN THE PRELIMINARY DESIGN PHASE**

Odeh Dababneh¹
Department of Aerospace Eng., Middle East
Technical University
Ankara, Turkey

Altan Kayran²
Department of Aerospace Eng., Middle East
Technical University
Ankara, Turkey

ABSTRACT

In this article, semi-monocoque wing structures are optimized for minimum weight by using different one and two dimensional element pair combinations, which are typically used to model the sub-elements of semi-monocoque wing structures, in the finite element models. The main objective of the study is to investigate the effect of using different one and two dimensional finite element pairs in the finite element models on the optimized configurations of the wing structure, and propose alternative optimized initial wing configurations to be considered as starting points in the detailed structural design phase. During the optimization study, structural optimization is performed by the coarse and fine mesh finite element models, and the effect of mesh size on the optimized wing configurations is studied. Optimization of the wing structures are performed by employing both continuous and discrete variable optimization. In case of optimization of wing structures with many design variables, it is very probable that local optimum designs may be reached if different starting values are used for the design variables during the optimization. Therefore, the effects of different starting points, as well as the effect of relaxing the constraints, on the optimized wing configurations are also investigated. The effect of using different one and two dimensional element pairs on the final optimized configurations of the wing structure is investigated, and conclusions are inferred with regard to the sensitivity of the optimized wing configurations with respect to the choice of different element types in the finite element model. Final optimized wing structure configurations are also compared with the simplified method based designs which are also optimized iteratively.

KEYWORDS: Structural Optimization, Wing Structure, Finite Element Analysis, Preliminary Design

INTRODUCTION

Optimization methods are used in the structures area in many engineering fields for a long time. Achieving minimum weight design, while satisfying certain constraints is the most common strategy that is followed in structural optimization. Weight saving in aerospace structures is becoming ever more significant.

¹ Grad. Student, e132180@metu.edu.tr

² Prof. Dr., akayran@metu.edu.tr

Thin walled lifting surfaces are regions where substantial weight savings can be achieved if optimization techniques are used early in the design phase. In recent years, structural optimization has been combined with finite element analysis to size structures that may minimize weight subject to a number of constraints. In the literature, one can find a large number of references in the area of structural optimization. A number of key studies were carried out in the field of optimization methods and their use in structural engineering areas. One review article is the work of Wasiutynski and Brandt who conducted a study in the field of optimum design of structures in 1960s [16]. In the area of optimum structural design concepts for aerospace vehicles Gerard presented a generalized approach for optimum design theory and preferred methods of presenting optimum design results [15]. The paper by Ashley gives an excellent re-view on the use of optimization in aeronautical engineering [13]. Another study on the subject of optimization of wing structures presented by Richard Butler who presented an overview of some of the existing optimization methods which may be applied at various stages during the design of wing structures [8]. Traditional modeling approach of aerospace structures, which are characterized by very thin elastic sheets and stiffeners, is to use shear panels to model thin sheets and use rod elements to account for the extensional behavior of the stringers. In general, to model thin walled shell structures three main element types may be used. These elements are shear panel, and shell elements having only membrane or only bending or both membrane and bending behavior [5]. Revised formulation of shell elements, which takes the drilling degrees of freedom into account, are also used depending on the external loading condition. On the other hand, stringers or spar caps may be modeled with beam or rod elements. The correct use of the element types is linked very closely to the loading condition. Many commercial finite element programs have built-in optimization modules which work in conjunction with their finite element solvers. For instance, optimization module of MSC Nastran [4] utilizes the DOT optimization algorithms from Vanderplaats Research and Development Inc.[2]. MSC Nastran employs a number of techniques, which are referred to as approximation concepts, to make design optimization possible for large finite element models. A more thorough literature survey on the optimization of wing structures is given by Ekren and Kayran [7].

In the present study, structural optimization is performed by MSC Nastran using different combinations of two dimensional and one dimensional finite element pairs, which are used to model sub-elements of wing structures. Present article deals with property optimization, therefore, location of spars, stringers and ribs are taken as constant and shape optimization is not considered. Wing structures are optimized with the objective of minimizing the weight of the wing while satisfying stress, deflection and local buckling constraints, and a number of side constraints are used to drive the optimizer towards the optimum solution faster. With the present study, it is intended to investigate the effect of using different elements on the final optimized configuration of the wing structure, and to infer conclusions with regard to the sensitivity of the optimized wing configuration with respect to the choice of different element types in the finite element model. During the optimization study, the effect of design constraints on optimum wing configurations is also evaluated by relaxing certain constraints such as deflection and local buckling. Optimization of the wing structures are performed by employing both continuous and discrete variable optimization. The discrete variable optimizations methods, which are available in MSC Nastran, are also compared with each other in one case study. Final optimized wing structure configurations are also compared with the simplified method based designs which are also optimized iteratively in another study.

OPTIMIZATION PROCESS IN MSC.NASTRAN

Design optimization capability of MSC Nastran is composed of two parts. The first part is the analysis model, in which grid locations, element structure and properties, material information, loads, boundary conditions and load cases are described. The second part is the design model which defines the design variables, relates the design variables to element properties, defines the design responses, and describes constraints and objectives in the design model. The initial design is the input to the MSC.NASTRAN® optimization process. In MSC.NASTRAN® optimization process, a finite element analysis is performed first and for design sensitivity and optimization, it is frequently necessary to perform multiple analyses. The constraint screening activity refers to the process that is used to identify those constraints that are likely to drive the redesign process. In another words by the constraint screening activity those constraints that are violated or likely to be violated are identified. These are set to be as active constraints. Sensitivity analysis is always performed automatically in MSC.NASTRAN® whenever design optimization is requested. Design sensitivity analysis computes the rates of change of structural response quantities or a change in constraint values with respect to

changes in design variables. MSC.NASTRAN® uses the DOT optimization code in the background as the optimizer [2]. The approximate model is constructed by using the information from finite element analysis and sensitivity analysis. This model involves the construction of high-quality approximations to the finite element results so that the number of full scale finite element analyses is kept to a minimum. Optimizer performs optimization process by using the approximate model. By default, gradient based method is used to construct the improved design. Other available methods are sequential linear programming and sequential quadratic programming. The improved model is the point at which the finite element model is updated based on the results from the optimizer so that a new finite element analysis is started. The improved model is compared with the previous model and if the changes are below the desired value, this means that soft convergence is achieved. Then, after the finite element analysis, one more convergence test for hard convergence is performed. Detailed information about MSC.NASTRAN® sensitivity analysis and optimization process is given in Reference [4]. However, it would be worthwhile to overview the approximation concepts used in structural optimization in more detail. The optimizer programs need frequent function evaluations to calculate design responses and response derivatives to calculate design sensitivities. Therefore, the cost of optimization becomes very high if traditional optimization approach is followed which is depicted in Figure 1.

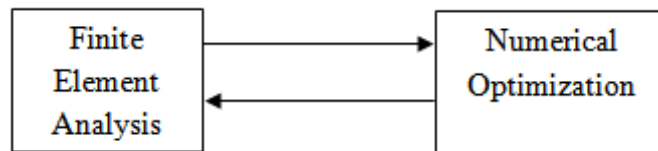


Figure 1. Traditional optimization approach

The traditional approach of optimization, as it can be seen from Fig. 1, involves request for a finite element analysis whenever the optimizer needs function evaluations. Therefore, in most design problems unless the problem is small in scale, the traditional approach tends to be useless. To overcome this major drawback, MSC Nastran employs concepts that limit the number of required finite element analysis. These concepts are named as approximation concepts used in structural optimization and they can be grouped into three major categories.

Design variable linking:

Design variable linking refers to narrowing the design task to that of determining the best combination of just few of design variables. It becomes much more efficient to link design variables if possible. That is, it would be advantageous if all the design variables could be varied in a suitably proportional manner according to the changes made to a much smaller set of independent variables. In Nastran this task is established by the user.

Constraint Screening:

Another concept which is employed by MSC Nastran that simplifies the numerical optimization process is to delete constraints which are not critical. In order to achieve constraint deletion, constraints that are violated or nearly violated must be identified. These constraints which are likely to be violated are the ones which derive the design. Constraint deletion allows the optimizer to consider a reduced set of constraints, and also reduces the computational effort associated with determining the required structural response derivatives.

Approximate Design Model:

Once the constraint set that seems to be deriving the design is identified, the next step that MSC Nastran follows is to perform parametric analysis in order to determine how these constraints vary as the design is modified. A parametric study is carried out with formal approximations, or series expansions of response quantities in terms of design variables. Formal approximations make use of the results of sensitivity analysis to construct an approximation to the true design space. Although formal approximations are locally valid, they are explicit in the design variables. The resultant explicit representation can then be used by the optimizer whenever function or gradient evaluations are required, instead of the costly implicit finite element analysis. The use of the approximate model is illustrated in Figure 2. Finite element model forms the basis for creation of the approximate models

which is subsequently used by the optimizer. The approximate model includes the effect of design variable linking, constraint deletion, and formal approximations. Constraint deletion and formal approximations are performed automatically in MSC Nastran [4]

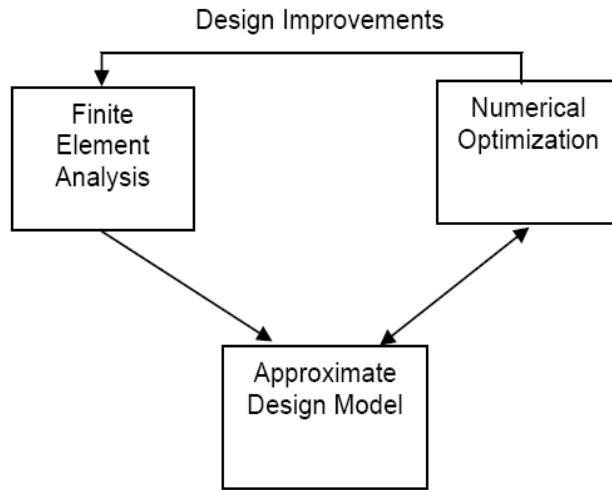


Figure 2. Coupling finite element analysis and optimization using approximate design model [4]

Once a new design has been proposed by the optimizer, based on the information supplied by the approximate model, in the next step a detailed analysis is performed of the new configuration to see if it has actually managed to satisfy the various design constraints and make improvement in the objective function. The upper segment denoted by ‘Design Improvements’ in Figure 3 represents the re-analysis update of the proposed designs. If a subsequent approximate optimization is needed, the finite element analysis serves as the new baseline from which to construct another approximate sub-problem. This cycle may be repeated as necessary until convergence is achieved, and these loops are referred to as design cycles in MSC Nastran [4]. Expanded version of Figure 2 is given in Figure 3. MSC Nastran utilizes the DOT optimization algorithm from Vanderplaats R&D, Inc. [2]. As Figure 3 shows, the optimizer interacts with the approximate model rather than the finite element model and produces an improved design. Once the improved design is obtained, the finite element model is updated based on the results from the optimizer so that a new finite element analysis can be performed.

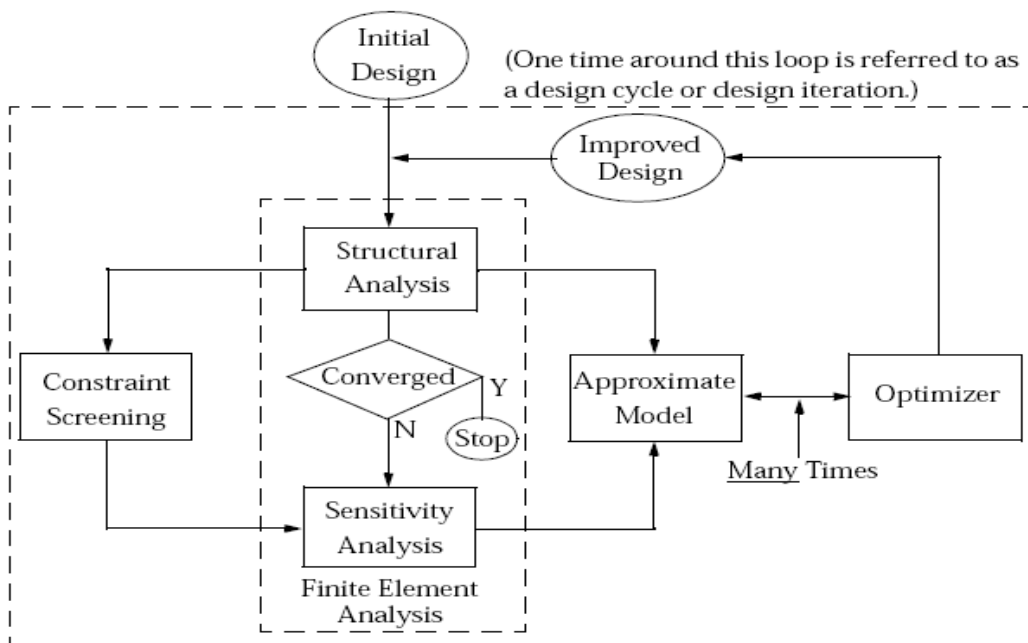


Figure 3. MSC.NASTRAN® Implementation of Structural Optimization [4]

A key part of the implementation of the optimization process is to determine when to stop the iterations. There are two levels at which convergence is tested. The lower level is at the optimizer level, and it is at this level where the optimizer decides on the optimized solution based on the output of the approximate model. The second and higher level is with respect to the overall design cycles. Figure 3 shows the locations of higher level of convergence tests. As shown in Figure 3 hard convergence compares the most recent finite element analysis with those from the previous design cycle. Since this test compares exact results from two consecutive analyses, it is named as hard convergence. This test is used as the default test for determining whether or not to terminate the design-cycle process. On the other hand soft convergence compares the design variables and properties output from the approximate optimization with those of the input to the approximate optimization. If design variables and properties have not changed appreciably, another finite element analysis may not be asked for.

OPTIMIZATION METHODS IN MSC.NASTRAN

Optimization problems can generally be described as either continuous or discrete, but may be a mix of both. MSC.NASTRAN® Sol 200 supports comprehensive structural design optimization for continuous design variables and also has the ability to apply discrete variables in the optimization process. This is done in recognition of the fact that practical engineering considerations frequently dictate that values of the designed properties be chosen from a discrete set. While the variables in continuous optimization problems are allowed to take on any values permitted by the constraints, discrete optimization is concerned with the case where the variables may only take on discrete values. MSC.NASTRAN® developed and implemented approaches to deal with discrete variables with limited computational cost. Design of Experiments (DOE) and Conservative Discrete Design (CDD) approaches together with engineering round-off and round-up methods, can be used to process discrete variables at any specified continuous design optimization cycle for structural design problems [4, 6]. The discrete optimization methods are briefly reviewed.

A. Round-Up and Round-Off Discrete Variable Processing Methods

These two methods are applied simply by rounding up or down the continuous solution obtained from solving a corresponding continuous optimization problem. These two methods have been implemented in MSC. Nastran® for quick discrete design solutions. These methods simply automate the simple rounding process a user might employ after a continuous optimization and require no new analyses.

B. Conservative Discrete Design (CDD) Variable Processing Method

The CDD approach is employed to quickly obtain a conservative discrete solution based on the continuous optimal solution and by using the sensitivity information values. For the CDD method, each variable is independently set to the discrete values that bracket the continuous variable result. An approximate analysis is carried out for the discrete variable above the continuous value and one with the discrete variable below the continuous value. The constraint results of these two analyses are compared and the discrete variable is chosen that gives the minimum value for the maximum constraint. This is repeated for each design variable so that $2 \cdot \text{nndv}$ (where nndv is the number of design variables that can take on discrete sizes) approximate analyses are carried out for the CDD approach. The advantages of CDD methods is that it may be used for a design with large number of discrete variables, and it is able to produce better discrete solution than round-off method.

C. Design of Experiments (DOE) Variable Processing Method

The DOE approach aims to obtain a good discrete design by evaluating the approximate objective and constraints with extra but limited computational cost. The implementation of DOE employed in MSC. Nastran employs an exhaustive search when nndv (the number of design variables that can take on discrete sizes) is 2^{16} or less. Above this value, an Orthogonal Array concept is employed to select candidate arrays that provide a representative sampling of the overall design space. The continuous optimal design obtained from current SOL 200 is used instead of the initial design model as a baseline for discrete variable processing. DOE assumed that the discrete optimum is close to the continuous optimum, and it is expected that a discrete solution by the DOE be close to the discrete optimum due to the selected design baseline. Therefore, searching a feasible discrete design is emphasized in the DOE processing. A major advantage of the DOE is its simplicity in applications, non-gradient

methodology, and ability to handle discrete variables. More detail information and discussion about DOE can be found in References [6, 10].

STRUCTURAL OPTIMIZATION OF THE WING STRUCTURE

The wing structure that is used in optimization is assumed to be for a single utility aircraft having a maximum take-off weight of 1460 kg and minimum operating weight of 861 kg. The wing structure is straight and unswept, and has a NACA 2412 airfoil profile with a rectangular planform, with a chord length of 1.524 m and semi-span of 4.572 m. Wing structural optimization is done for a two-spar, two-stiffener and seven-rib configuration dividing the wing into 6 equal sections of length 0.762 m. The root extensions of the front and rear spars are of 0.5 m in length. The front spar is located at 25 % of the chord length; the rear spar is located at 70% of the chord length, and the upper and lower stiffeners are located respectively at 50 % and 46% of the chord length. Figure 4 shows the wing model with the spars, stiffeners and ribs that is used in the optimization study.

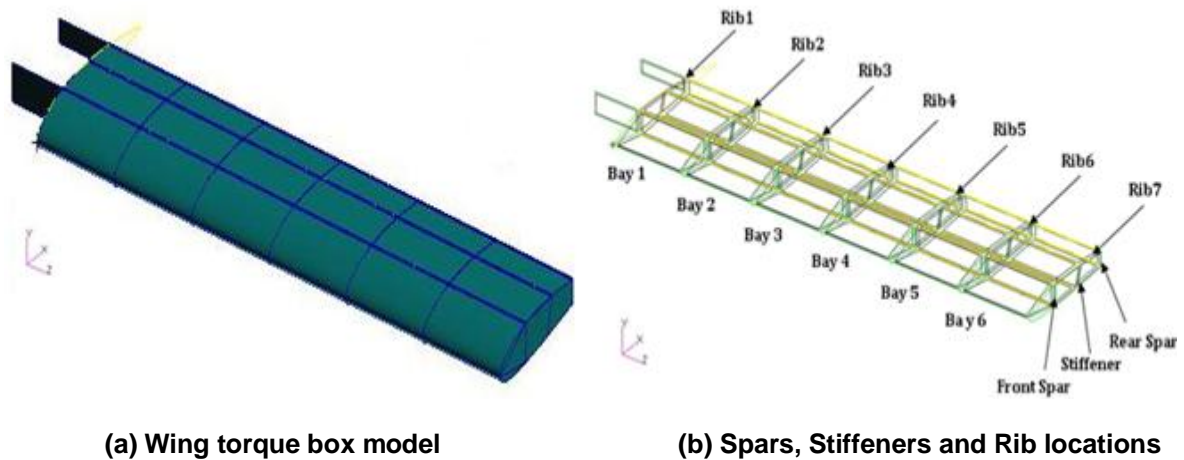


Figure 4. Wing model used in the optimization study

External Aerodynamic Loading Acting on the Wing

The aerodynamic loading is distributed to the wing structure in a discrete fashion by calculating equivalent force components at the 25 % of the chord length. The calculation of the external aerodynamic load is performed using the code provided by ESDU, ESDUpac A9510 attached in ESDU 95010 [11]. Lift force and pitching moment are considered as line loading, and they are distributed along the lower front spar as shown in Fig.5. Wing is fixed at wing root extensions, which are not considered in the optimization process.

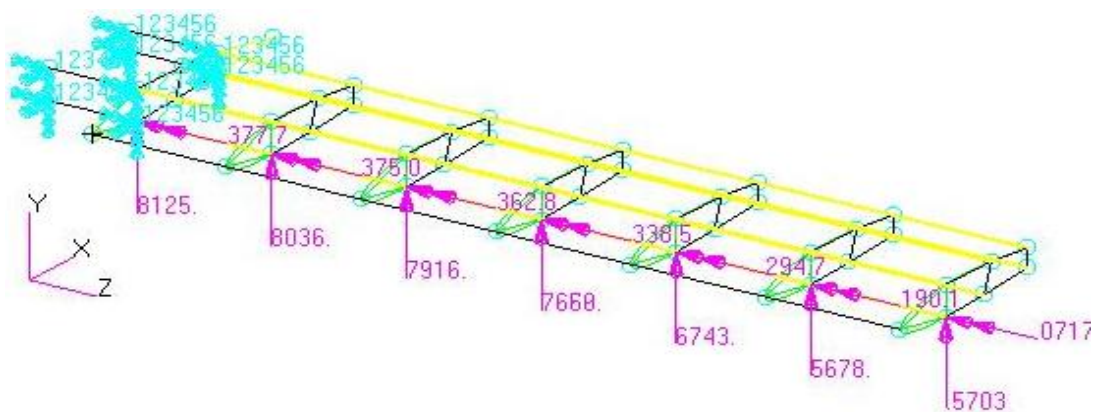


Figure 5. Distribution of the external aerodynamic loading

DESCRIPTION OF THE OPTIMIZATION STUDY

A. Methodology

This section introduces the finite element models of the wing structure which are generated by using different one and two dimensional element pairs. The main objective of using different one and two dimensional finite element models is to investigate their effect on the final optimized configuration of the wing structure and also to make comparisons between the final optimized results obtained by these different models. Table 1 summarizes the element pairs that are used to model the one dimensional and the two dimensional members of the wing structure.

Table 1. Combination of element types used in modeling the wing structure

Model	Thin Walled Panels	Spar Caps and Stringers
1	Shell Element (CQUAD4)	Rod Element (CROD)
2	Shell Element (CQUAD4)	Beam Element (CBAR)
3	Shell-R Element (CQUADR)	Rod Element (CROD)
4	Shell-R Element (CQUADR)	Beam Element (CBAR)
5	Membrane-R Element (CQUADR)	Rod Element (CROD)
6	Membrane-R Element (CQUADR)	Beam Element (CBAR)

Shell and membrane elements with –R extension are the so-called revised elements of Nastran which also have drilling degrees of freedom. It should be noted that the distributed line lift and pitching moment loading necessitates the use of revised membrane elements in the wing ribs, because with the standard membrane elements in the wing ribs, the distributed pitching moment cannot be handled accurately. In addition, in order to handle the distributed line lift and pitching moment accurately, in the finite element models with revised membrane elements, single elements must be used between the rib stations

B. Definition of the optimization problem

The wing torque box structural optimization deals with property optimization, therefore, location of spars, stringers and ribs are taken as constant and shape optimization is not considered in this study. The wing torque box optimization problem is defined as:

Objective Function:

- Minimize the weight of the wing torque box.

Constraints:

Stress Constraints:

- Von-Misses stresses in skins, spar webs and ribs: The lower limit is unconstrained; the upper limit is constrained with a maximum value of 322 MPa which is used as the allowable stress in the current study.
- Axial stresses of spars and stiffeners: The lower limit is constrained with a compression stress value of 322 MPa (-322 Mpa), and the upper limit is constrained with a tensile stress value of 322 MPa.

Deflection Constraints:

- The maximum tip displacement of the wing torque box is limited to 20 cm.

Local Buckling Constraints:

Local buckling equations are defined by design equations and entered externally to the MSC. Nastran input file.

- Buckling of skin panels is assumed to be due to combined shear stress and compression axial stress.

$$R_S^2 + R_C \leq 1 \Rightarrow \left(\frac{\tau}{K_S E \left(\frac{t}{b}\right)^2} \right)^2 + \left(\frac{\sigma_{Compression}}{K_C E \left(\frac{t}{b}\right)^2} \right) \leq 1 \quad (1)$$

- Buckling of spar webs is due to combined bending and shear stress.

$$R_S^2 + R_B^2 \leq 1 \Rightarrow \left(\frac{\tau}{K_S E \left(\frac{t}{b}\right)^2} \right)^2 + \left(\frac{\sigma_{Compression}}{K_B E \left(\frac{t}{b}\right)^2} \right)^2 \leq 1 \quad (2)$$

- Buckling of ribs due to shear stress only.

$$\frac{\tau}{K_S E \left(\frac{t}{b}\right)^2} \leq 1 \quad (3)$$

The lower limit is unconstrained; the upper limit is constrained with a maximum value of 1.01.

Geometric or Side Constraints:

Side constraints are added to the definition of the optimization problem so as to drive the optimizer towards an optimum solution which makes sense from an engineering point of view. It should be noted that since the external load decreases from root to tip, and in the load case no local concentrated forces are considered along the span of the wing, side constraints drive the optimizer in the correct direction towards optimum solution. Side constraints are again externally defined by writing design equations in the input file.

Constraints on Thicknesses of Thin Walled Panels:

- Thicknesses of skin and web panels and ribs are forced to decrease bay by bay from the root to the tip of the wing in a discrete fashion. No thickness variation is allowed in a bay. Design equations relating the thicknesses are defined and entered externally to the MSC. Nastran input file. Such a constraint definition is necessary because in the gradient based optimization of wing torque box, it is very likely that the solution reached is a local optimum solution. In the analyses carried out, it is experienced that in some of these local optimum solutions, thicknesses of some inboard thin panels turned out to be smaller than the thicknesses of some outboard thin panels. Because in the gradient based solution, if the optimum solution is stuck around a local optimum, it may not get around it all the time, and in such cases such strange results are obtained. Therefore, in the present study, design equations are written in the input file such that thicknesses of the thin walled panels are forced to decrease from wing root to wing tip. Thus, the optimizer is derived towards an optimum solution which makes sense from an engineering point of view.

Constraints on Spar Cap and Stiffener Areas:

- Spar cap and stiffeners areas are forced to decrease bay by bay from the wing root to the tip of the wing in a discrete fashion. No area variation is allowed in a bay. Equations relating areas are defined by design equations and entered externally to the MSC. Nastran input file. The same reasoning that is written for the thicknesses is also valid here.

Design Variables:

- For the finite element models which have flanges and stringers modeled with rod elements, 92 design variables are used which represent the thicknesses of wing skins, and spar webs, ribs, and spar flange and stringer areas.
- For the finite element models which have flanges and stringers modeled with beam elements, 128 design variables are used which represent the thicknesses of wing skins, and spar webs, ribs, and beam height and widths. In beam modeling of spar flanges and stringers, it is assumed that beams have rectangular cross-sections. In the discrete solution, beam heights are selected from the standard thickness lists assuming that spar caps and stringers are cut from standard size sheets, whereas continuous optimum solutions are used for the beam widths since beam widths, which are cut from thin sheets, can be adjusted to be any continuous value.

Design variables associated with the thicknesses of thin walled panels:

- Seven Nose Rib Thicknesses
- Seven Mid rib Thicknesses
- Six Front Spar Web Thicknesses
- Six Rear Spar Web Thicknesses
- Six Nose Skin Thicknesses
- Six Upper Mid-Skin Thicknesses
- Six Lower Mid-Skin Thicknesses
- Six Upper Rear (Right) -Skin Thicknesses
- Six Lower Rear (Right) -Skin Thicknesses

Figure 6 illustrates the rendered coarsest mesh finite element wing model and shows the two dimensional elements which are used to model the rib webs ,skin panels and spar webs.

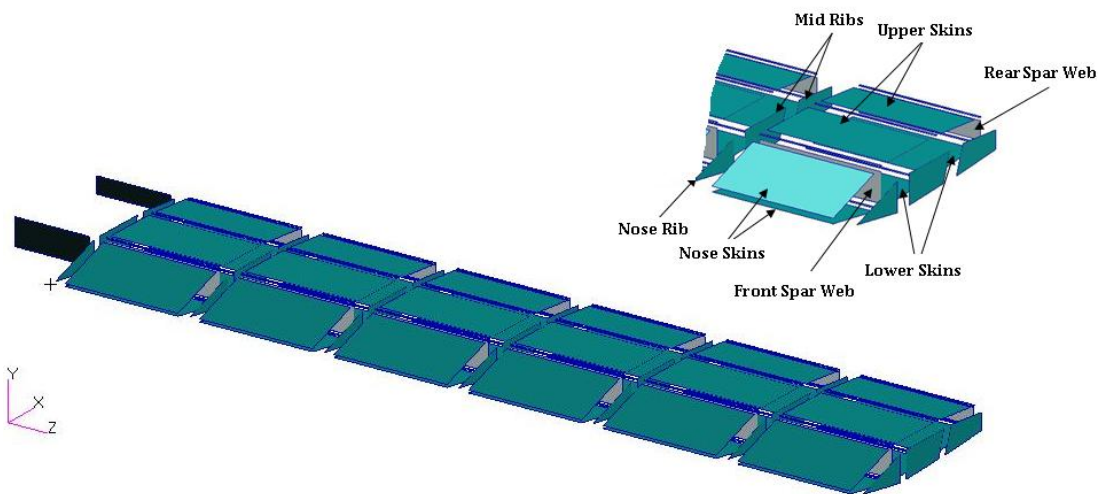


Figure 6. Rendered Finite Element Model of the Wing

Design variables associated with the areas of spar caps and stiffeners:

(When Rod Elements are used):

- Six Front Spar Upper Cap Areas
- Six Front Spar Lower Cap Areas
- Six Rear Spar Upper Cap Areas
- Six Rear Spar Lower Cap Areas
- Six Upper Skin Mid Stiffener Areas
- Six Lower Skin Mid Stiffener Areas

(When Beam Elements are used):

- Twelve Front Spar Upper Dimensions (Width and Height)
- Twelve Front Spar Lower Dimensions (Width and Height)
- Twelve Rear Spar Upper Dimensions (Width and Height)
- Twelve Rear Spar Lower Dimensions (Width and Height)
- Twelve Upper Skin Mid Stiffener Dimensions (Width and Height)
- Twelve Lower Skin Mid Stiffener Dimensions (Width and Height)

In the optimization process, all the thicknesses are assumed to have a lower limit of 0.0003 m and an upper limit of 0.00635 m. The caps areas of spars and stiffeners are assumed to be rectangular areas in the case of using rod elements with a lower limit of 0.000038 m² and an upper limit of 0.000613 m². In the case of using beam elements, lower limit of the width is assigned as 0.02 m and the upper limit of the width is taken as 0.15 m and no discrete values are assigned for it since the width is assumed to be cut from a thin sheet. Since any value between 0.02 - 0.15 m can be assigned as the width of the beam, width of the beam is a continuous design variable. On the other hand, beam height is taken as a discrete design variable and it is assumed that beam height is the same as the thickness of the standard thickness thin sheets. In the optimization process, the lower limit of the beam height is taken as 0.0003 m and the upper limit is taken as 0.00406 m. The lower and upper limits of the thicknesses and flange/stiffener areas are taken as the lower and upper limits of the standard thicknesses and flange/stiffener areas [1, 9, 14]. The standard sheet thicknesses and flange areas are given below.

Thin Panels Thicknesses Set {0.3, 0.4, 0.5, 0.63, 0.81, 1.016, 1.27, 1.20, 1.80, 2.03, 2.28, 2.54, 3.17, 4.06, 4.82, 6.35} × 10⁻³ m

Flange Cross Sectional Areas Set {38, 44, 48, 58, 63, 67, 73, 78, 88, 94, 98, 104, 108, 112, 116, 118, 131, 133, 137, 148, 151, 153, 161, 184, 195, 213, 232, 246, 280, 312, 375, 390, 415, 430, 444, 525, 573, 592, 613} × 10⁻⁶ m²

Beam Heights Dimensions Set {0.3, 0.4, 0.5, 0.63, 0.81, 1.016, 1.27, 1.20, 1.80, 2.03, 2.28, 2.54, 3.17, 4.06} × 10⁻³ m

It should be noted that in applying the stress constraints for the skin and the web panels in a bay, for the fine mesh models, maximum stresses in the related domains are checked against the allowable stress value. In a bay, related domains are the skin and web panels shown in Fig.4, ribs and spar flange and stringer lines extending from one rib station to the other. On the other hand, for the local buckling constraints, average stresses in the thin walled panels are used to calculate the stress ratios to be used with the interaction equations used in local buckling checks under combined loading.

OPTIMIZATION RESULTS USING DIFFERENT STARTING VALUES FOR DESIGN VARIABLES AND USING DIFFERENT DISCRETE OPTIMIZATION METHODS

A. Optimization results using different starting values for design variables

In case of optimization of wing torque box with many design variables, it is very probable that local optimum design may be reached if different starting values are used for the design variables during the optimization. Therefore, the effect of different starting points on the optimized wing configuration is investigated in this section. The wing torque box is optimized by using rod-shell model with coarse mesh and using different starting points for the design variables. Again the objective function was to minimize the weight of the wing subjected to Von Mises stress, axial stress, tip deflection and local buckling constraints. Both continuous and discrete round-up solutions are conducted. The models with different starting values for design variables are defined as follow:

Model 1: Initial values are taken as lower limit of the design variables

Model 2: Initial values are taken as mean of the lower and upper limit of the design variables

Model 3: Initial values are taken as upper limit of the design variables

Model 4: Initial values decrease by 10% for each bay starting from the maximum values at the root bay

Model 5: Initial values decrease by 20% for each bay starting from the maximum values at the root bay

Model 6: Initial values are taken as the values of the simplified method of solution obtained using the second structural idealization

Table 1 shows the mass of optimized wing torque box using the same rod-shell model, but using different starting values for the design variables. In all solutions, hard convergence is achieved as well as hard feasible discrete design.

Table 1 Mass of optimized wing torque box (kg) using different starting values for design variables

Mass of optimized wing torque box (Kg)		
Model	Continuous	Discrete - Round Up
Model-1	41.03 kg	45.93 kg
Model-2	40.09 kg	45.10 kg
Model-3	41.29 kg	45.94 kg
Model-4	39.85 kg	44.32 kg
Model-5	39.80 kg	44.00 kg
Model-6	41.09 kg	46.77 kg

Table1 reveals that using different starting values for design variables, in the gradient based optimization problem, can lead to the local optimum designs, since the optimized wing configurations do not exactly have the same weights. However, the change in weights among the models is small for both continuous and discrete optimization solutions. Moreover, using the results determined by hand calculation (default results) as the starting values for the design variables during optimization; satisfactory solution is also obtained which is evident from the results given in Table 1.

B. Optimization study results using different discrete optimization methods

In this section, the wing torque box is optimized by using rod-shell model with coarse mesh and using the discrete optimization methods described in previous sections of the present article. The goal is to understand and examine the effect and correct use of discrete optimization methods available in MSC.NASTRAN®. The objective function is to minimize the weight of the wing subjected to Von Misses stress, axial stress, tip deflection and local buckling constraints. Both continuous and discrete optimization solutions are conducted. Table 2 shows the mass of optimized wing torque box using the same rod-shell model, but using different discrete methods.

Table 2 Mass of optimized wing torque box (kg) using MSC.NASTRAN® different discrete optimization method

Mass of optimized wing torque box (Kg)		
Method	Continuous	Discrete
DOE	41.09 kg	44.81 kg
CDD	41.09 kg	42.62 kg
Round Up	41.09 kg	46.77 kg
Round Off	41.09 kg	40.03 kg

A hard convergence solution at an optimum value is achieved using four different discrete optimization methods but feasible discrete designs are obtained only for the DOE and the Round-Up methods. On the other hand, CDD method could not obtain a feasible discrete solution. The reason might be due to fact that while the CDD method tries to produce a true conservative design, it neglects the interaction of discrete variables such that the approximations may not be accurate enough to find a feasible design. The Round-off method could also not obtain a feasible discrete solution, since it uses simple rounding down from the continuous solution obtained from solving a corresponding continuous optimization problem which requires no new analyses. Therefore, the chance of finding a feasible solution becomes smaller, since the round-off method also neglects the effect of the interaction of discrete variables.

In the article, the remaining discrete optimum solutions are determined by the round-up method based on the continuous solution obtained after solving the continuous optimization problem.

STRUCTURAL OPTIMIZATION RESULTS OF THE WING STRUCTURE USING SIX DIFFERENT FINITE ELEMENT COMBINATIONS

A. Wing torque box optimization results including all design constraints

In this section the wing torque box configurations given in Table 1 are optimized for minimum weight with all the design constraints included and for both coarse and fine mesh models. The effect of using different element types in the finite element model on the optimized wing torque box configurations is investigated, and the effect of mesh size on the final optimum configurations is studied by employing

finite element models, with different mesh densities. During the optimization process, hard convergence is achieved as well as hard and soft feasible discrete designs. Tables 3 and 4 show the masses of the optimized wing structures, obtained using different finite element combinations, given in Table 1, including all the design constraints. In Tables 3 and 4, optimized masses for the coarse and fine mesh cases, and the masses of the wing found by another study of the authors using simplified method of analysis based on unsymmetric beam theory utilizing two different structural idealizations are also given. The two different structural idealizations can briefly be described as [12, 14, 17]:

Design criteria for structural idealization 1 (skins and webs carry shear load only and spar flanges and stringers carry axial stress)

- Maximum shear stresses in the skins and webs of each bay should be less than the shear stress allowable
- Maximum axial stress in the spar flange and stringers should be less than the stress
- Local shear buckling of the wing skins and spar webs in each bay should be prevented

Design criteria for structural idealization 2 (skins and webs carry shear and axial load and spar flanges and stringers carry axial stress)

- Maximum Von-Misses stresses in the skins and webs of each bay should be less than the stress allowable
- Maximum axial stress in the spar flange and stringers should be less than the stress allowable
- Combined tension and shear local buckling of the lower wing skins should be prevented
- Combined compression and shear local buckling of the upper wing skins should be prevented
- Combined bending and shear local buckling of the spar webs should be prevented

Table 3. Optimized masses of the wing structure – Coarse mesh results

Model	Mass of optimized wing torque box (Kg)		
	Initial	Continuous	Discrete Round Up
Rod/Shell	65.38 kg	41.09 kg	46.77 kg
Beam/Shell	65.38 kg	38.28 kg	42.97 kg
Rod/Shell-R	65.38 kg	38.88 kg	43.57 kg
Beam/Shell-R	65.38 kg	38.29 kg	42.11 kg
Rod/Membrane-R	65.38 kg	39.01 kg	44.07 kg
Beam/Membrane-R	65.38 kg	37.77 kg	42.84 kg
Simplified Method ¹	-----	52.18 kg	57.61 kg
Simplified Method ²	-----	62.90 kg	67.69 kg

¹ Structural idealization 2

² Structural idealization 1

Table 4. Optimized masses of the wing structure – Fine mesh results

Model	Mass of optimized wing torque box (Kg)		
	Initial	Continuous	Discrete Round Up
Rod/Shell	66.67 kg	51.50 kg	58.61 kg
Beam/Shell	66.67 kg	50.25 kg	58.02 kg
Rod/Shell-R	66.67 kg	50.12 kg	58.23 kg
Beam/Shell-R	66.67 kg	52.13 kg	59.70 kg
Simplified Method ¹	-----	52.18 kg	57.61 kg
Simplified Method ²	-----	62.90 kg	67.69 kg

¹ Structural idealization 2

² Structural idealization 1

From Tables 3 and 4 it is clear that the initial mass of the fine mesh finite element models is slightly higher than the initial mass of the coarse mesh finite element models, because cambered surfaces of the wing is approximated better with the fine mesh.

It should be noted that in the discrete optimization, MSC Nastran is allowed to select the first round-up dimensions among a list of standard thicknesses and flange areas. Therefore, masses determined by the discrete optimization are higher than the masses determined by the continuous optimization. On the other hand, for each 1D and 2D element combination shown in Tables 3 and 4, the optimized mass of the wing torque box obtained using the fine mesh model in the optimization process, is higher than the optimized mass of the wing torque box obtained using the coarse mesh model. It should be noted that although the stresses at the centers of the domains of the bays are lower for the fine mesh models, maximum stresses of the fine mesh models in the domains of each bay are higher than the maximum stresses obtained by the coarse mesh models in the optimization process. For the coarse mesh case, the stresses at the element centers of the shell and bar elements are used in the stress constraint equations. Therefore, for the coarse mesh case, stresses at the element centers correspond to the mid bay locations. However, for the fine mesh case, stress constraints are written with respect to the maximum stress in the domains of each bay. Therefore, fine mesh models have higher stresses because maximum stress in a bay is at the inboard end of the bay. Thus, approximately there is 10 kg difference between the optimized masses of the wing torque boxes obtained by the coarse and fine mesh finite element models in the optimization process. However, the effect of local buckling and maximum deflection constraints should also be checked to confirm this conclusion.

Results of the optimization study shows that optimized wing masses, determined by the use of the different finite element models in the optimization process, are very close to each other with only slight favorable overall mass on behalf of models which have spar flanges and stringers meshed with beam elements.

The mass of the wing configuration designed by the simplified method using the second structural idealization is very close to the optimized masses determined by the use of fine mesh finite element models in the optimization process. However, simplified method of analysis using the second structural idealization is more comparable to the structural analysis performed by the coarse mesh finite element models. From Table 3 it is seen that mass of the wing configuration designed by the simplified method using the second structural idealization has approximately 10 kg mass penalty compared to the optimized masses determined by the coarse mesh finite element models. It should be noted that results of the simplified method of analysis have been obtained by iterating over the standard thicknesses and standard flange areas, thus in a way, they are also optimized values. Therefore, optimized masses obtained by the use of the second structural idealization are very encouraging in terms of the applicability of the simplified method of analysis in the design and optimization of wing structures in the preliminary design stage.

From the results given in Tables 3 and 4, it is seen that the standard shell elements and revised shell elements results in slightly different minimum mass wing configurations. However, the difference between the optimized masses is small. It is noticed that in the continuous optimization solution, in general, the use of shell elements with drilling degrees of freedom results in slightly lower minimum masses compared to the use of shell elements without drilling degrees of freedom. In the analysis study of the authors, it is noted that in general finite element analysis of the wing torque box with revised shell elements results in slightly lower stresses compared to the use of standard shell elements in the finite element model. Therefore, it can be concluded that results of the continuous optimization solution is in accordance with the stress analysis results.

Results given in Table 3 also shows that the use of membrane elements, with drilling degrees of freedom, in the finite element model gives optimized masses which are very close to the optimized masses determined with finite element models having standard or revised shell elements. Therefore, it can be concluded that the use of revised formulation membrane elements in the coarse mesh finite element models is justified in structural optimization problems. However, in the coarse mesh models single elements are used between the rib stations, accuracy issue is still there.

As a sample solution, Figures 7 and 8 show the history of the objective function, which is the total mass of the wing, with respect to design cycles for rod/shell model for the coarse and the finest mesh cases, respectively. Both hard and soft convergences are achieved in 15 design iterations for the coarse mesh and in 18 design iterations for the fine mesh models. For both coarse and fine mesh models, mass versus design iteration curves level out and converged solutions are achieved. Continuous optimization for the coarse mesh case is achieved in 14 design iterations but the last iteration corresponds to the round-up discrete solution. Similarly, continuous optimization for the finest mesh case is achieved in 17 design iterations. In the round-up method, continuous solutions for the design variables are rounded-up to the first values in the standard size list for the design variables. Therefore, in Figures 7 and 8, the increase in the objective function value corresponds to the discrete solution obtained by using the round-up method.

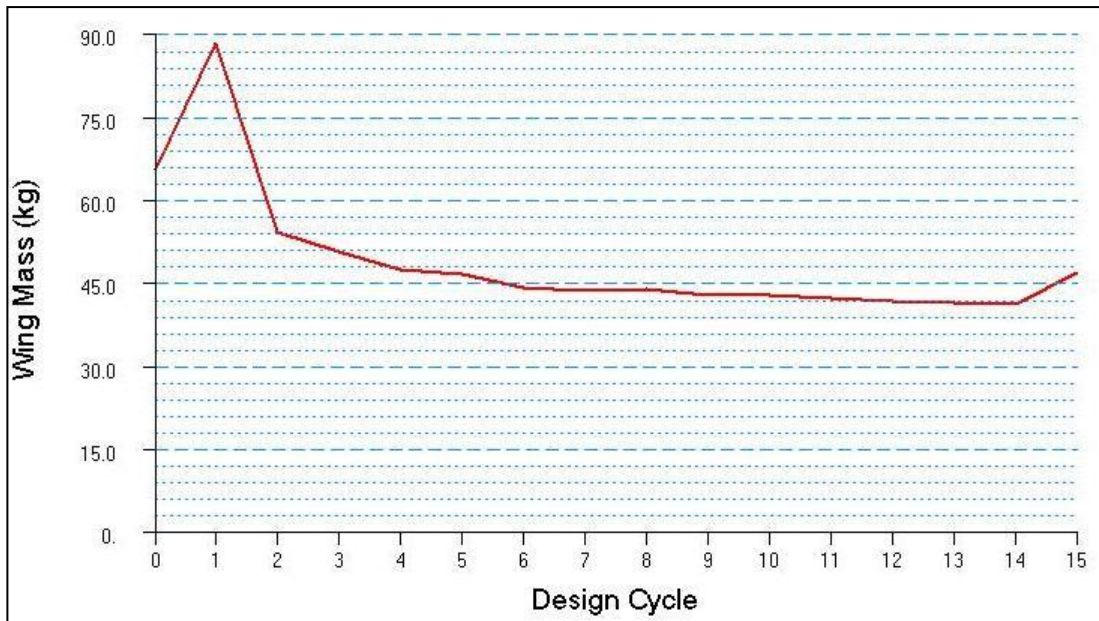


Figure 7. Variation of the mass of wing with respect to design cycles – coarse mesh rod-shell model

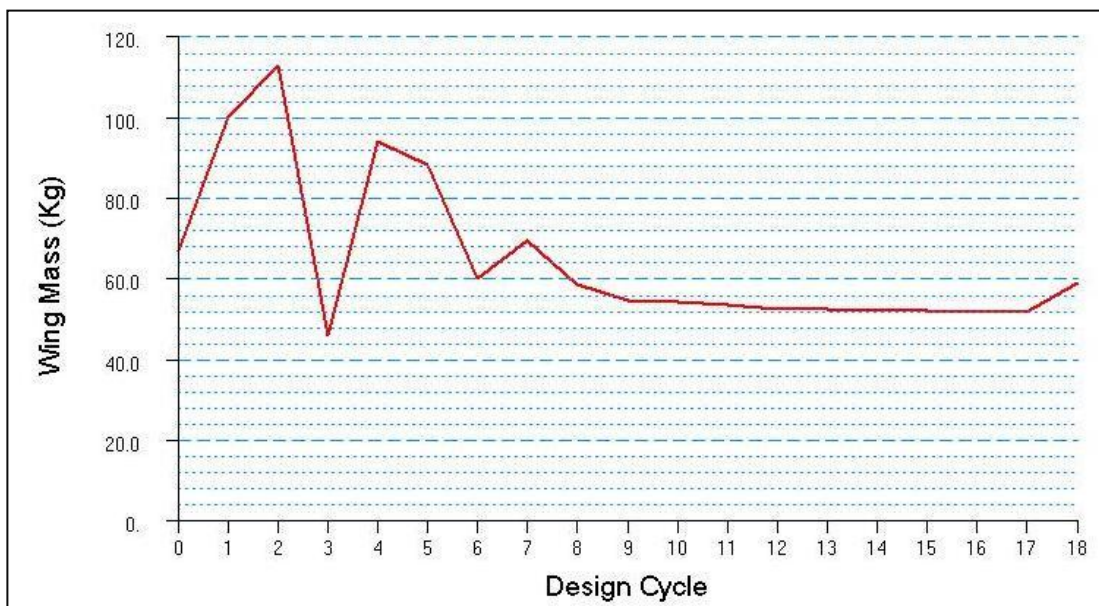


Figure 8. Variation of the mass of wing with respect to design cycles – fine mesh rod-shell model

Figures 9 and 10 show the thickness scalar plots of the lower skin, spar web and rib panels, in the optimized wing structure which is modeled with rod/shell element combination for the coarse and the fine mesh models, respectively. It must be noted that these scalar plots refer to the results of discrete optimization solution. From the scalar plots, it can be seen that thicknesses of the panels decrease from the root to the tip of the wing, as expected. It should be reminded that the decrease of the thicknesses of skin/web/rib panels from the wing root to wing tip is specified as the side constraints. The solutions given in Figures 9 and 10 verify that the side constraints work fine, and thicknesses decrease from wing root to wing tip.

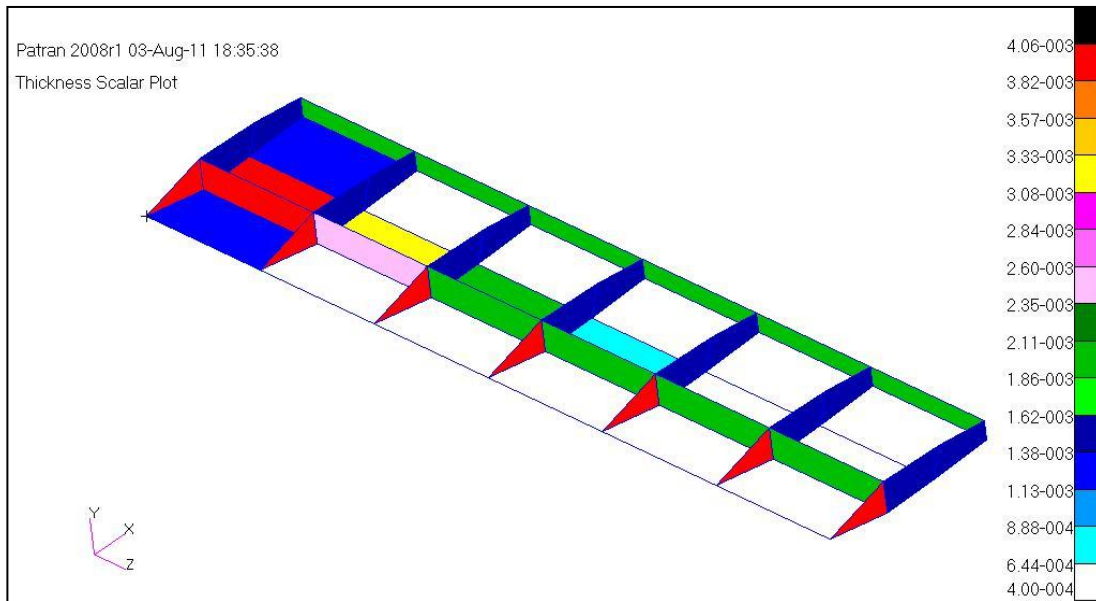


Figure 9. Thickness scalar plots of lower skin, spar web and rib panels in the optimized wing torque box - coarse mesh rod/shell model

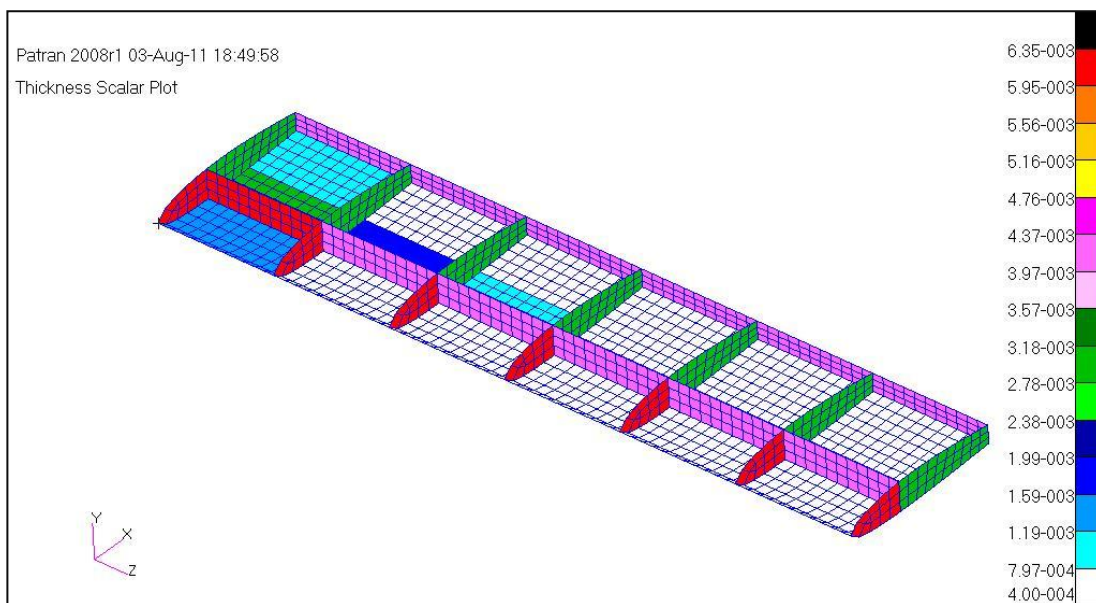


Figure 10. Thickness scalar plots of lower skin, spar web and rib panels in the optimized wing torque box - fine mesh rod/shell model

Table 5 summarizes the spar cap areas of the front spar in the optimized rod/shell wing torque box model for both the coarse and fine mesh models. From Table 5, it is seen that spar caps cross sectional areas decrease from the root to the tip of the wing, as expected. The fine mesh model results in larger spar caps areas since when the mesh is made finer, maximum axial stresses in the spar and stringer domains in each bay increase, and inevitably the spar cap areas also increase to satisfy the axial stress constraints defined for one dimensional members.

Table 5. Upper and lower flange areas of the front spar of the wing – rod/shell model

Front Spar Cross Sectional Area – Rod /Shell Model					
	Spar Cap (Root to Tip)	Coarse Mesh Model		Fine Mesh Model	
		Continuous Area (m ²)	Discrete Area (m ²)	Continuous Area (m ²)	Discrete Area (m ²)
Upper Flange	Bay 1	2.75E-04	2.80E-04	6.13E-04	6.13E-04
	Bay 2	4.15E-05	4.40E-05	5.20E-04	5.25E-04
	Bay 3	4.03E-05	4.40E-05	2.61E-04	2.80E-04
	Bay 4	4.03E-05	4.40E-05	6.81E-05	7.30E-05
	Bay 5	3.80E-05	4.40E-05	3.80E-05	4.40E-05
	Bay 6	3.80E-05	4.40E-05	3.80E-05	4.40E-05
Lower Flange	Bay 1	6.13E-04	6.13E-04	6.13E-04	6.13E-04
	Bay 2	4.16E-05	4.40E-05	4.65E-04	5.25E-04
	Bay 3	4.00E-05	4.40E-05	2.43E-04	2.46E-04
	Bay 4	3.96E-05	4.40E-05	6.80E-05	7.30E-05
	Bay 5	3.80E-05	4.40E-05	3.80E-05	4.40E-05
	Bay 6	3.80E-05	4.40E-05	3.80E-05	4.40E-05

B. The Effect of Design Constraints on Optimum Wing Structure Configurations

The effect of design constraints on optimum wing configurations is evaluated by relaxing certain constraints such as deflection and local buckling. In this section one of the wing torque box configurations (rod-shell model) is optimized for minimum weight while considering the effect of each constraint individually on the optimum design mass of the wing. The rod/shell model of the wing is optimized using the coarse and the fine mesh finite element models under the following constraints:

- Case 1- Stress constraints only
- Case 2- Stress and tip displacement constraints only
- Case 3- Stress and buckling constraints only

Tables 6 and 7 give the masses of the optimized wing torque box obtained under different design constraints, for the coarse and the fine mesh cases, respectively. The first row of Tables 6 and 7 give the optimized masses for the full set of constraints including the stress, displacement and local buckling.

Table 6. Effect of constraints - Coarse Mesh Results

Constraints	Initial Mass(kg)	Continuous Optimization(kg)	Discrete Optimization(kg)
Stress+deflection+buckling	65.38	41.09	46.8
Stress	65.38	17.95	21.10
Stress+deflection	65.38	31.94	37.63
Stress+buckling	65.38	30.20	34.76

Table 7. Effect of constraints - Fine Mesh Results

Constraints	Initial Mass(kg)	Continuous Optimization(kg)	Discrete Optimization(kg)
Stress+deflection+buckling	66.67	51.50	58.61
Stress	66.67	26.84	30.37
Stress+deflection	66.67	34.63	38.57
Stress+buckling	66.67	45.51	51.72

As it can be seen from Tables 6 and 7, optimization of wing torque box under stresses constraint only results in optimized masses which are significantly small when compared to the optimized masses for the rod/shell model with all the constraints included. The main reason for the large difference is due to relaxing the local buckling and tip deflection constraints in the optimization problem. Table 6 and 7 also show that optimized masses determined by the use of fine mesh finite element models in the optimization process are higher than the optimized masses determined by the use of coarse mesh finite element models in the optimization process. Since for the particular optimization problem only stress constraints are used, with confidence it can be concluded that higher maximum stress of the fine mesh models in the domains of each bay is the main reason for the higher optimized mass obtained by the use of fine mesh model in the optimization process.

By introducing the displacement constraint besides the stress constraint, the difference between the optimized masses determined by the coarse mesh and the fine mesh models become less when it is compared to the results under stress constraint only. Compared to the results of the optimization problem with stress constraints only, for the combined stress and displacement constraint problem, the increase of the optimized mass of the coarse mesh model is much higher than the increase of the optimized mass of the fine mesh model. This result is an indication that displacement constraint is a more stringent constraint for the coarse mesh model compared to the fine mesh model.

Table 7 shows that for the fine mesh case, buckling constraint besides stress constraint results in higher optimized mass compared to the optimized mass obtained under stress and displacement constraints. This result is an indication of that local buckling is a much more stringent constraint than the deflection constraint for this particular problem. However, for the coarse mesh model, optimization using the stress and deflection constraints results in slightly higher mass than the optimization under stress and buckling constraints. This result is an indication of the significant effect of the mesh size on the optimum mass configurations. Since results of fine mesh finite element models are more reliable, it can be concluded that coarse mesh finite model underestimates the effect of local buckling constraint on the optimum mass configuration.

CONCLUSION

In the present article, the effect of using different one and two dimensional element pairs in the finite element models on the optimized configurations of the wing structure is investigated. Structural optimization results showed that optimized wing masses, determined by the use of different finite element models in the optimization process, are very close to each other with only slight favorable overall mass on behalf of models using beam elements in the axial members. It is also observed that in the continuous optimization solution, in general, the use of shell elements with drilling degrees of freedom results in slightly lower optimum masses compared to the use of shell elements without drilling degrees of freedom. However, differences are negligible from an engineering point of view.

Optimized masses obtained with the fine mesh finite element models are higher than the optimized masses obtained with the coarse mesh finite element models. It should be noted that although the stresses at the centers of the domains of bays are lower for the fine mesh models, the maximum stresses in the domains of each bay are higher in the fine mesh finite element models. In the optimization solution, maximum stresses in the domains are used in the stress constraint equations. Therefore, when fine mesh finite element models are used in the optimization process, optimized masses turn out to be higher than the optimized masses obtained by the use of coarse mesh finite element models in the optimization process.

The mass of the wing configuration designed by the simplified method using the second structural idealization is very close to the optimized masses determined by the finite element based optimization process performed by MSC Nastran. Based on the preliminary results presented in the current study, it can be concluded that with the simplified methods, preliminary sizing of the wing configurations can be performed with enough confidence as long as the simplified method based designs are also optimized.

REFERENCES

- [1] Aircraft Spruce and Specialty Co., <http://www.aircraftspruce.com>, last accessed date on 10th January 2011
- [2] Vanderplaats R&D, DOT Optimization Software <https://www.vrand.com/contact.html>, last accessed date 13 March 2011
- [3] Howe, D., *Aircraft Loading and Structural Layout*, AIAA Publication, VA, USA, 2004.
- [4] MSC.NASTRAN® 2005 r3, "Design Sensitivity and Optimization User's Guide", MSC Software Corp., 2003
- [5] Schaeffer, H.G., *MSC.Nastran Primer for Linear Static Analysis*, MSC Software Corporation, Santa Ana, California 2001. p.184—191, pp.289-306.
- [6] Xiaoming Yu, Erwin H. Johnson, and Shenghua Zhang. Discrete Optimization in MSC Nastran. MSC Software Corporation, Costa Mesa, CA 92626, September 2000
- [7] Ekren, M. and Kayran, A., *Structural Optimization of Wing Torque Boxes Using Different Structural Idealizations in the Finite Element Model*, Journal of Spacecraft, Proceedings of the 5th. Ankara International Conference, Ankara, Turkey, 17-19 August, 2009, METU, Ankara, in CD ROM.
- [8] Butler, R., *The Optimization of Wing Structures*, Aircraft Engineering and Aerospace Technology, Vol.70, No. 1, 1998, pp. 4-8.
- [9] MIL-HDBK-5H: Military Handbook Metallic Materials and Elements for Aerospace Vehicle Structures, Department of Defense, USA, December 1998
- [10] Lee, K.H. and Park, G.J., "Discrete Post Process of the Constrained Size Optimization Using Orthogonal Arrays", AIAA-96-3987-CP, 6th AIAA/NASA/ISSMO Symposium on Multidisciplinary Analysis and Optimization, Bellevue, WA, September 4-6, 1996
- [11] ESDU 95010, *Computer program for estimation of span-wise loading of wings with camber and twist in subsonic attached flow*, <http://www.esdu.com>, June 1995.
- [12] Megson, T.H.G., *Aircraft Structures for Engineering Students*, Second edition, John Wiley and Sons, New York, USA, 1990.
- [13] Ashley, H., *On Making Things the Best-Aeronautical Uses of Optimization*, Journal of Aircraft, Vol. 19, No.1, 1982, pp. 5-28.
- [14] Bruhn, E.F., *Analysis and Design of Flight Vehicle Structures*, Tri-State Offset Company, USA, 1973.
- [15] Gerard, G., *Optimum Structural Design Concepts for Aerospace Vehicles*, Journal of Spacecraft, Vol.3, No.1, 1966, pp. 5-18.
- [16] Wasiutynski, Z., and Brandt, A., *The Present State of Knowledge in the Field of Optimum Design of Structures*, Applied Mechanics Reviews, Vol. 16, No.5, 1963, pp. 341-350.
- [17] Peery, D.J., *Aircraft Structures*, McGraw Hill, First Edition, New York, USA, 1950.